Available online at www.sciencedirect.com
SCIENCE DIRECT
Thermochimica Acta 446 (2006) 66–72
thermochimica acta
www.elsevier.com/locate/tca

# High pressure differential scanning calorimetry: Aspects of calibration

J. Ledru [a,*], C.T. Imrie [a], J.M. Hutchinson [b], G.W.H. Höhne [c]

[a] *School of Engineering and Physical Sciences, University of Aberdeen, Aberdeen AB24 3UE, UK*
[b] *Departament de Màquines i Motors Tèrmics, Universitat Politècnica de Catalunya, 08222 Terrassa, Spain*
[c] *Department of Polymer Technology, Eindhoven University of Technology, 5600 MB Eindhoven, The Netherlands*

Available online 7 May 2006

Dedicated to Professor Wolfgang Hemminger on the occasion of his 65th anniversary.

**Abstract**

A high pressure differential scanning calorimeter (HP-DSC) based on an original design of Höhne and co-workers has been constructed at the University of Aberdeen to allow the characterisation of the thermal behaviour of materials under pressure in both fundamental and technological research areas, for example, in the offshore and pharmaceutical industries. The HP-DSC is equipped with an autoclave using silicone oil as the pressurising medium and may be operated in a temperature range from 20 °C to 300 °C at pressures from 0.1 MPa to 500 MPa and with various heating and cooling rates (from 0.5 K min$^{-1}$ to 20 K min$^{-1}$). For calibration purposes, the pressure dependence of the melting temperatures and associated enthalpy changes of both indium and tin have been investigated and compared to the data obtained by Höhne and co-workers for indium and from other published data in the literature for tin. From the heat flow calibration, a dimensionless enthalpy correction factor $R_{corr}(p)$ has been determined which may be used to correct the measured enthalpy values over the whole temperature range and for any given pressure value. Likewise a calibration diagram has been constructed from the temperature calibration over the full range of pressure up to 500 MPa to allow the corrected temperature to be determined from the measured temperature for a thermal event occurring at any pressure.


*Keywords:* High pressure differential scanning calorimeter; Calibration; Pressure dependence; Heat of fusion; Melting temperature

## 1. Introduction

Differential scanning calorimetry is the most widely used thermal analytical technique, but is used almost exclusively under ambient pressure conditions. Indeed commercial "high pressure differential scanning calorimeters" (HP-DSC) operate at rather moderate pressures of up to 40 MPa. The characterisation of the thermal behaviour of materials under high pressure is, however, clearly of both fundamental and technological importance. In the offshore industry, for example, temperatures of 200 °C and pressures of 200 MPa are routinely encountered. It is important therefore to be able to measure important material parameters under such conditions.

To address this surprising omission in available instrumentation, some 15 years ago Höhne designed and built a high pressure differential scanning calorimeter [1,2] and used it to characterise a number of polymeric materials [2–9]. Other techniques developed later or used more recently to characterise materials under pressure include pressure differential scanning calorimetry (PDSC) [10,11] and high pressure MicroDSC [12], though the maximum pressure available from these techniques is in the range 3–40 MPa, high pressure differential thermal analysis [13], high pressure dielectric spectroscopy [14–17] and scanning transitiometry or PVT scanning calorimetry [18–22], PVT experiments [23–25] and conductivity measurements [26–30], while studies have also been made at ambient pressure, for example, by DSC, on samples prepared under high pressure [31–34].

HP-DSC is both a fast and, after careful calibration, accurate method which provides complementary and important information to these techniques and hence we have constructed a HP-DSC in Aberdeen based on Höhne's design.

This paper briefly reviews the design of the new HP-DSC system and presents, for the first time, the whole procedure needed to calibrate the instrument carefully. This necessarily includes a precise measurement of the pressure dependence of the melting temperatures and associated enthalpy changes of both indium

* Corresponding author. Tel.: +44 1224274349; fax: +44 1224272921.
*E-mail address:* j.ledru@abdn.ac.uk (J. Ledru).

0040-6031/$ – see front matter © 2006 Elsevier B.V. All rights reserved.
doi:10.1016/j.tca.2006.04.018

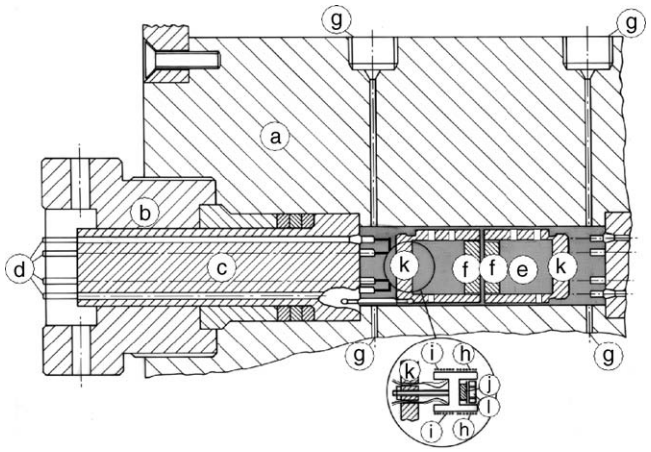


Fig. 1. Schematic cross-section drawing of the autoclave and of one of the furnaces showing: (a) the autoclave body, (b) end cap, (c) plugs containing (d) leads through, (e) silicone oil, (f) screw caps, (g) oil entry, exit and pressure transducer locations, (h) platinum resistance heater, (i) sensor windings on silver former, (j) sample in aluminium crucible, (k) glass ceramic housings with leads through and with holes on the bottom for oil entry and on the top for oil and air escape and (l) furnace lid with holes in the left-hand side ceramic housing; there is an identical reference furnace, in reverse, in the right-hand side ceramic housing. In this drawing, only the sample furnace is shown on the left-hand side screw cap.

and tin and we compare these data to those obtained by Höhne et al. [35].

## 2. Experimental

The design of our HP-DSC apparatus is based upon that developed by Blankenhorn and Höhne [1] and Höhne [2] (Fig. 1). The HP-DSC operates on the power compensation principle, making use of a Pyris Diamond DSC (Perkin-Elmer), and is equipped with an autoclave which can be pressurised by means of a hand-operated spindle pump, with silicone oil as the pressurising medium (Fig. 2). The complete high pressure system, including the autoclave (Fig. 2(j)), the spindle pump (Fig. 2(d)), high pressure lines, valves and transducers (Fig. 2(e–h)), was provided by SITEC-Sieber Engineering AG. The HP-DSC head consists of two self-contained silver furnaces located within ceramic housings (Fig. 1(k)), which themselves closely fit within the autoclave (Fig. 1). The furnaces were constructed by the Eindhoven University of Technology, with platinum wire windings for both the heaters and sensors (Fig. 1(h and i), respectively) to match the resistance of the Pyris DSC cell, and with leads through the autoclave closing caps (Fig. 1(b–d)) to the Pyris control system. The platinum wires were insulated from each other and from the silver furnaces by means of ceramic glue.

Using a branched silicone oil of approximately 100 mPa s viscosity (Wacker-Chemie GmbH Wacker® AS 100), the HP-DSC may be operated in a temperature range from 20 °C to 300 °C at pressures from 50 MPa to 500 MPa and with various heating and cooling rates (from 0.5 K $min^{-1}$ to 20 K $min^{-1}$). The actual pressure value within the autoclave is measured using a pressure transducer (Figs. 1(g) and 2(h)) close to the reference cell and connected to a data logger (Fig. 2(p)). Using the data logger leads to a relative uncertainty of 0.75% on the measured pressure value over the whole pressure range.

The hydrostatic pressure is transmitted to the sample inside the ceramic housing through holes in the ceramic housing (Fig. 1(k)) and inside the furnace through holes in the furnace lid (Fig. 1(l)). Thus, the sample (Fig. 1(j)) is completely surrounded by the pressurising medium but is encapsulated air-free in sealed aluminium crucibles to avoid contact with the pressurising medium (Fig. 1(j)). In operation, the ceramic housings are placed within the autoclave with their axes horizontal, and the furnace therefore has a lid (Fig. 1(l)) which screws down onto the crucible, ensuring that it is firmly located within the silver

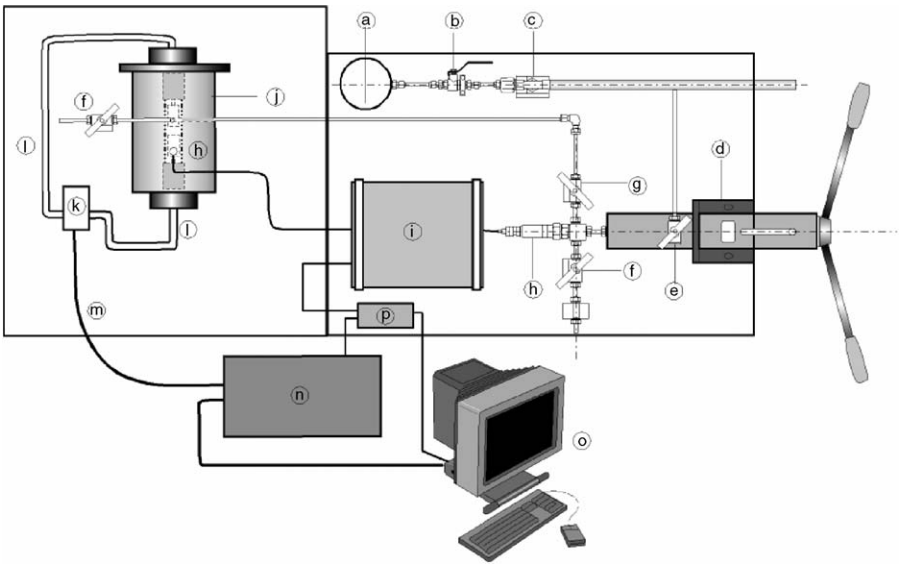


Fig. 2. Schematic presentation of the system showing: (a) oil reservoir, (b) ball valve, (c) prime pump, (d) high pressure spindle pump, (e) pump valve, (f) bleed valves, (g) high pressure isolator valve, (h) pressure transducers, (i) digital pressure display unit, (j) autoclave, (k) electrical connection box, (l) electrical leads from sensors and heaters, (m) electrical leads to the electronic board of the DSC, (n) DSC, (o) computer and (p) data logger.

furnace and that good thermal contact is made. The heater and sensor are well insulated on the outside of the furnace (Fig. 1(h and i), respectively); however, because of the excellent thermal conductivity of the silver, any thermal event in the sample will be recorded rapidly by the sensor with a corresponding rapid change in the power delivered to the heaters in order to maintain the programmed temperature, with unavoidable but small heat transfer to the surrounding oil [1,2]. The time constant of the cell is comparable to that of the platinum furnace used in the Perkin-Elmer DSC.

All calibration measurements were made on samples of about 18 mg using a non-calibrated HP-DSC. The heat (enthalpy) calibration was made only with indium for which the pressure dependence of both the melting temperature and the heat of fusion has been determined by high pressure dilatometry and high pressure differential scanning calorimetry leading to the best value estimation [35].

For the two-point temperature calibration over the given range of pressures, both indium and tin standards were used because the pressure dependence of their melting temperature has been determined for both [35–37]. In the temperature calibration experiments using indium (or tin), a sample of indium (or tin) was placed in both the sample and reference cells to determine the necessary correction for both cells. As will be seen, this allows online calibration to be performed during any subsequent experiment.

## 3. Results and discussion

### 3.1. Heat calibration

The first set of HP-DSC heating scans using just one indium sample in the sample cell is shown in Fig. 3. These scans were performed from 35 °C to 220 °C at 10 K min$^{-1}$ at pressures from approximately 50 MPa to 400 MPa, though only parts of the complete scans are shown in order to separate the curves more clearly. It should also be noted that the curves have been arbitrarily shifted by a small amount in the $y$-direction for clarity. In this figure, and in all the following figures showing HP-DSC heating scans, temperatures correspond to the measured sample temperatures and have not been calibrated.

Fig. 3 shows that the measured melting temperature clearly increases with pressure while the measured heat of fusion (peak area) is much less pressure dependent.

According to Höhne et al. [35], the best value for the pressure-dependent heat of fusion of indium may be estimated from their own results together with those from thermodynamic calculations assuming a pressure-independent entropy of fusion, and they give the following equation for what is referred to here as the reference heat of fusion of indium, $\Delta_{\mathrm{fus}}H^{\mathrm{In}}_{\mathrm{ref}}$:

$$\Delta_{\mathrm{fus}}H^{\mathrm{In}}_{\mathrm{ref}}\,(\mathrm{J\,g^{-1}}) = [\Delta_{\mathrm{fus}}H^{\mathrm{In}}_{0,\mathrm{ref}}\,(\mathrm{J\,g^{-1}})] + [(3.3 \pm 2) \times 10^{-3}\,(\mathrm{J\,g^{-1}\,MPa^{-1}})] \cdot [p\,(\mathrm{MPa})] - [(2.6 \pm 2) \times 10^{-7}\,(\mathrm{J\,g^{-1}\,MPa^{-2}})] \cdot [p\,(\mathrm{MPa})]^2 \quad (1)$$

where $\Delta_{\mathrm{fus}}H^{\mathrm{In}}_{0,\mathrm{ref}} = 28.62 \pm 0.11\,\mathrm{J\,g^{-1}}$ is taken as the best value for the heat of fusion of indium at normal pressure and $p$ is the pressure. The given standard deviations were defined from the best value estimation of the pressure dependence of the heat of fusion of indium. This leads to an uncertainty of 1.1 J g$^{-1}$ for the enthalpy of fusion of indium at 500 MPa.

The measured heat of fusion (determined from Fig. 3) is plotted as a function of pressure in Fig. 4, together with the best value function of Höhne et al. [35]. A least-squares fit to our data gives:

$$\Delta_{\mathrm{fus}}H^{\mathrm{In}}_{\mathrm{meas}}\,(\mathrm{J\,g^{-1}}) = [\Delta_{\mathrm{fus}}H^{\mathrm{In}}_{0,\mathrm{meas}}\,(\mathrm{J\,g^{-1}})] - [(2.7 \pm 1.9) \times 10^{-3}\,(\mathrm{J\,g^{-1}\,MPa^{-1}})] \cdot [p\,(\mathrm{MPa})] - [(1.6 \pm 4) \times 10^{-6}\,(\mathrm{J\,g^{-1}\,MPa^{-2}})] \cdot [p\,(\mathrm{MPa})]^2 \quad (2)$$

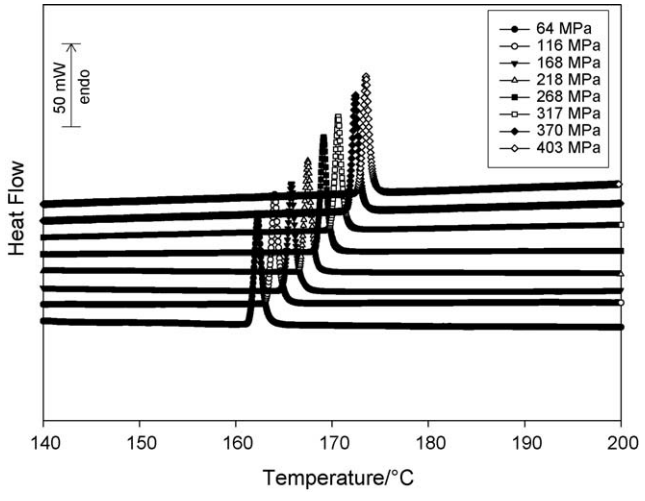


Fig. 3. HP-DSC heating scans at 10 K min$^{-1}$ and for various pressures obtained with one indium sample placed in the sample cell of the non-calibrated calorimeter. Note that only parts of the complete scans from 35 °C to 220 °C are shown here and that the curves have been arbitrarily shifted in the $y$-direction for clarity.

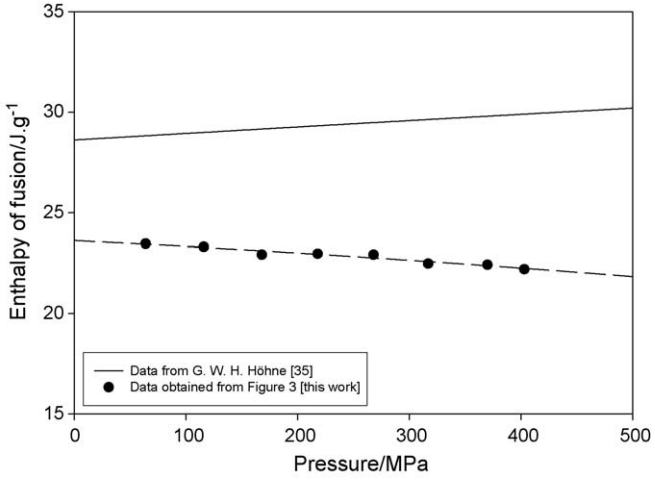


Fig. 4. Variation of the measured enthalpy of fusion of indium with pressure. The dashed line represents a least-squares fit to the data obtained from Fig. 3; the full line represents the best value data from Höhne et al. [35]. A dimensionless enthalpy correction factor $R_{\mathrm{corr}}$ (or calibration factor) is calculated from the ratio of these two curves.

for the pressure dependence of the measured heat of fusion $\Delta_{fus}H^{In}_{meas}$ of indium in our non-calibrated system, with $\Delta_{fus}H^{In}_{0,meas} = 23.62 \pm 0.20\,J\,g^{-1}$, the extrapolated measured value of the heat of fusion of indium at normal pressure and where $p$ is the pressure. The standard deviations were defined from the least-squares fit procedure and then lead to a maximum uncertainty of $2.0\,J\,g^{-1}$ for the measured heat of fusion of indium at 500 MPa. It can be seen from Fig. 4 that the heat of fusion of indium is rather independent of pressure.

The ratio of the reference and measured heat of fusion from Eqs. (1) and (2), respectively, provides a dimensionless enthalpy correction factor $R_{corr}(p)$ which may be determined for each pressure value. Then $R_{corr}(p)$ is simply given by:

$$R_{corr}(p) = \frac{\Delta_{fus}H^{In}_{ref}(p)}{\Delta_{fus}H^{In}_{meas}(p)} \quad (3)$$

Fig. 5 shows a plot of $R_{corr}(p)$ over the available range of pressure with a maximum uncertainty of 0.18 at 500 MPa.

This correction factor must be applied to all the measured peak area values over the temperature range used and at any given pressure to obtain a corrected enthalpy value $\Delta_{fus}H_{corr}(p)$ using:

$$\Delta_{fus}H_{corr}(p) = R_{corr}(p) \cdot \Delta_{fus}H_{meas}(p) \quad (4)$$

The pressure dependence of the heat of fusion for tin has not been reported, but as the heat of fusion of indium is much better known than the respective values for tin, there is no need to measure the pressure dependence of the heat of fusion of tin for the calibration of our power compensated DSC.

### 3.2. Temperature calibration

For temperature calibration, for both indium and tin standards, one sample was placed in the sample cell and another one in the reference cell, to calibrate both the sample and the reference cells and allow the possibility of verifying the temperature calibration online in any further investigations.

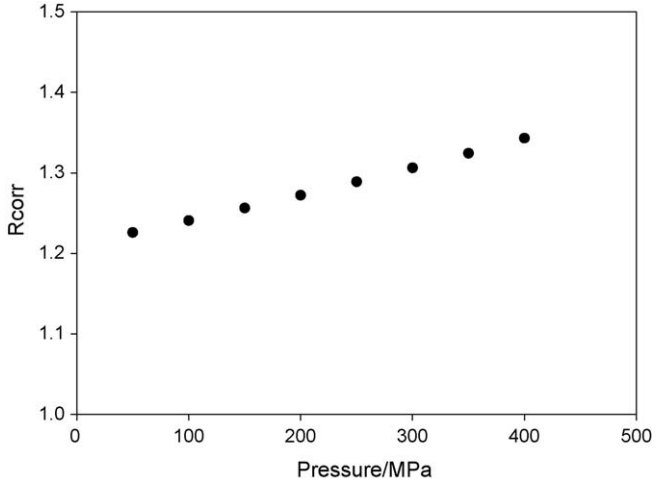


Fig. 5. Variation of the dimensionless enthalpy correction factor $R_{corr}$ with pressure.

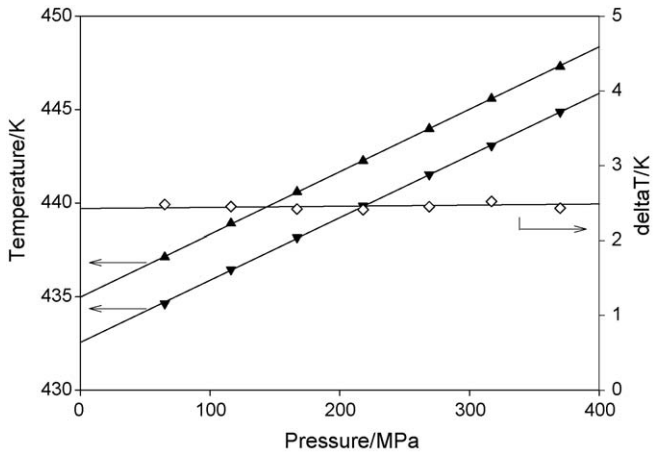


Fig. 6. Variations with pressure of the measured extrapolated onset temperature of the endothermic melting peak for a sample of indium in the sample cell (▼), of the measured temperature of the maximum of the "exothermic" melting peak of a sample of indium placed in the reference cell (▲) and of the difference in temperature between these two temperatures, $\Delta T$ (◊). The lines are drawn as a guide to the eye.

The HP-DSC heating scans obtained at $10\,K\,min^{-1}$ for pressures from 50 MPa to 400 MPa for indium (second set) and tin are not shown here but (as observed in Fig. 3 for the endothermic peak) both peak temperatures increase on increasing the pressure, but in such a way that the difference between the exothermic peak temperature, for the sample placed in the reference cell, and the extrapolated onset temperature of the endothermic peak, for the sample placed in the sample cell, $\Delta T$, remains constant (Fig. 6).

The dependence on pressure of the measured melting temperature (i.e. the extrapolated peak onset temperature from the sample cell) for indium and tin in the non-calibrated DSC is plotted in Figs. 7 and 8, respectively, together with the best value data obtained by Höhne et al. for indium [35] and the average of literature data for tin [36,37]. In Fig. 7, it can be seen that

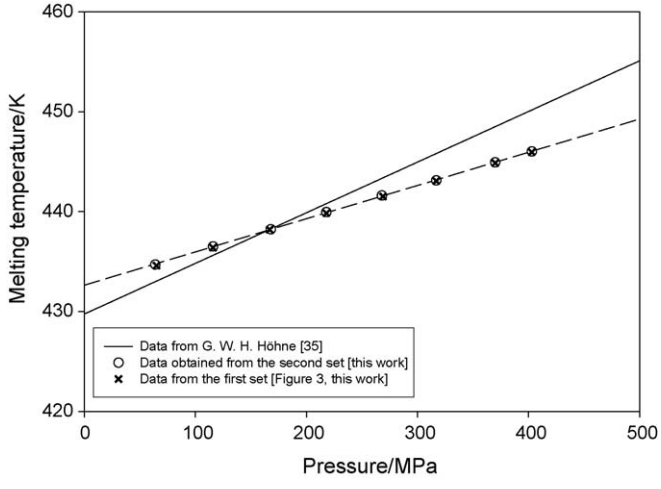


Fig. 7. Variation of the measured melting temperature of indium with pressure. The dashed line represents a least-squares fit to the data obtained from the first set of experiments (Fig. 3) and from the second set of experiments; the full line represents the best value data from Höhne et al. [35].

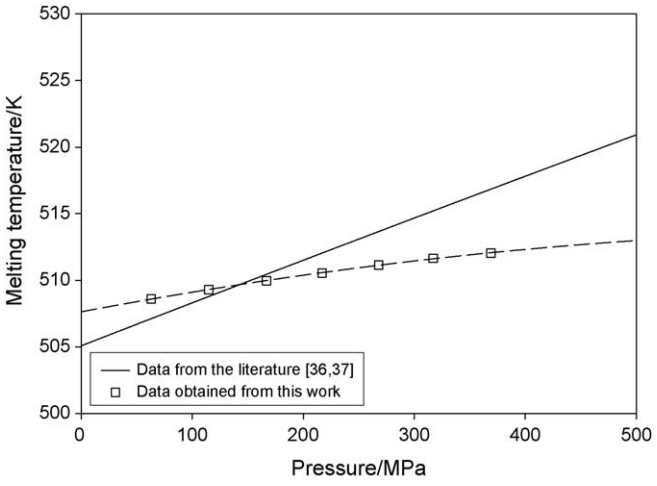


Fig. 8. Variation of the measured melting temperature of tin with pressure. The dashed line represents a least-squares fit to the data; the full line represents a fit function for the data from McDaniel et al. [36] and Sandrock [37].

the measured melting temperatures obtained for indium from two different sets of experiments (first set and second set) in the non-calibrated DSC are highly reproducible. Our measured data follow the same general behaviour as those obtained by Höhne et al. [35] for indium, and by McDaniel et al. [36] and Sandrock [37] for tin, though the both non-calibrated sets of data differ from the literature values. These deviations, as well as the difference observed for the pressure dependence of the heat of fusion of indium (Fig. 4), can be attributed to a number of possible factors (for example: small deviations of the resistances of the heater and sensor wires of the furnaces, unavoidable asymmetries between the cells, heat leakage from the furnaces to the surroundings, influence of pressure on the heating rate or on the thermal lag between the controlled furnace temperature and the sample temperature, etc.), but are also dependent on sample mass and heating rate; this justifies the need for a careful calibration of such a calorimeter.

For the pressure dependence of the melting temperature ($T_{fus}$) of indium, Höhne et al. [35] again give a best value estimation, being the average of their own experimental data and that of other workers, and including both dilatometric and calorimetric results. This best value estimation may be written:

$$T^{In}_{fus}(p)\,(K) = [T^{In}_{fus,0}\,(K)] + [(0.0507 \pm 0.0030)\,(K\,MPa^{-1})] \cdot [p\,(MPa)] \quad (5)$$

where $T^{In}_{fus,0} = 429.75$ K, the fixed melting point of the ITS-90 for indium at normal pressure [38], and $p$ is the pressure. The given standard deviation defines the limits of this best value estimation and leads to a maximum uncertainty of 1.5 K at 500 MPa.

The best fit line for our measurements with the non-calibrated DSC (Fig. 7) gives:

$$T^{In}_{fus,meas}(p)\,(K) = [T^{In}_{0,meas}\,(K)] + [(0.0333 \pm 0.0002)\,(K\,MPa^{-1})] \cdot [p\,(MPa)] \quad (6)$$

where $T^{In}_{0,meas} = 432.64 \pm 0.04$ K, the extrapolated measured melting temperature for indium at normal pressure and $p$ is the pressure. The estimated standard deviation defines the limits of our fit and leads to a maximum uncertainty of 0.1 K at 500 MPa.

For the pressure dependence of the melting temperature ($T_{fus}$) of tin, the following empirical temperature–pressure function was determined using the literature data [36,37]:

$$T^{Sn}_{fus}(p)\,(K) = [T^{Sn}_{fus,0}\,(K)] + [(0.0324 \pm 0.0025)\,(K\,MPa^{-1})] \cdot [p\,(MPa)] - [(1.45 \pm 4.86) \times 10^{-6}\,(K\,MPa^{-2})] \cdot [p\,(MPa)]^2 \quad (7)$$

where $T^{Sn}_{fus,0} = 505.08$ K, the fixed melting point of the ITS-90 for tin at normal pressure [38], and $p$ is the pressure. The standard deviations were defined from this best value estimation and lead to a maximum uncertainty of 2.5 K at 500 MPa for the literature data.

Applying a regression function to our tin data from the non-calibrated DSC gives:

$$T^{Sn}_{fus,meas}(p)\,(K) = [T^{Sn}_{0,meas}\,(K)] + [(0.0158 \pm 0.0006)\,(K\,MPa^{-1})] \cdot [p\,(MPa)] - [(10.11 \pm 1.32) \times 10^{-6}\,(K\,MPa^{-2})] \cdot [p\,(MPa)]^2 \quad (8)$$

where $T^{Sn}_{0,meas} = 507.63 \pm 0.05$ K, the extrapolated measured melting temperature for tin at normal pressure, and $p$ is the pressure. Again the standard deviations were defined from the best value estimation and then lead to a maximum uncertainty of 0.6 K at 500 MPa for the measured melting temperature of tin.

Whatever the measured deviations from the theoretical temperature–pressure functions are, Eqs. (5) and (6) for indium and Eqs. (7) and (8) for tin allow us to determine the proper temperature correction for our system ($\Delta T_{corr}$), defined as the reference temperature minus the measured temperature at each pressure for both indium and tin, where the reference values are defined by Eqs. (5) and (7) for indium and tin, respectively. This then permits the construction of a calibration diagram in which the $\Delta T_{corr}$ values are plotted against the measured temperature for both indium and tin, for pressures from 50 MPa to 500 MPa, as is shown in Fig. 9. In this figure, a linear relationship between the temperature correction and the measured temperature has been assumed, as is usual for two point calibration, to enable an extrapolation to be made over a wider temperature range. For the temperature correction, a maximum uncertainty of 1.6 K at 500 MPa has been calculated from Eqs. (5) and (6) from the indium values. For tin, the maximum uncertainty for the correction is larger, namely 3.1 K at 500 MPa.

Then, to calculate the corrected temperature from the measured temperature $T_{meas}$ for a given pressure, we use the linear correction field shown in Fig. 9 describing the variation of the temperature correction with the measured temperature for that particular pressure value. The corrected temperature ($T_{corr}$) is then calculated using:

$$T_{corr}(p, T) = T_{meas}(p, T) + \Delta T_{corr}(p, T) \quad (9)$$

The overall uncertainty of the corrected temperatures is within the range 1–4 K depending on temperature and pressure.

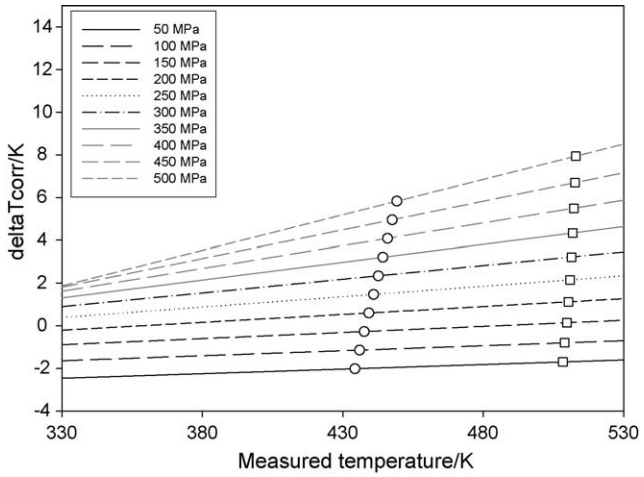


Fig. 9. Plot of the temperature correction as a function of the measured temperature (see text) for different pressure values: (◯) indium data and (□) tin data.

As noted already, a small indium sample may be placed in the reference cell to verify the temperature calibration online, and then Eq. (9) may be rewritten as:

$$T_{\text{true}}(p) = T_{\text{meas}}(p) + \Delta T_{\text{corr}}(p, T) + \Delta T_{\text{obs}} \quad (10)$$

where $\Delta T_{\text{obs}}$ is the difference observed between the maximum temperature of the "exothermic" melting peak of indium measured on any HP-DSC curve at any pressure value and the maximum temperature of the "exothermic" melting peak of indium for the same pressure value (since the difference between the maximum temperature of the "exothermic" melting peak and the onset temperature of the endothermic melting peak has been found to be pressure independent; Fig. 6).

It should be noted that this "online" verification procedure is not always appropriate and its application depends on the temperature range investigated and on whether thermal events are expected to occur in the temperature region of the indium melting.

Furthermore, under ideal circumstances, $\Delta T_{\text{obs}}$ will be zero. If it deviates significantly from zero, this implies that the calibration procedure based upon the derivation of the temperature correction $\Delta T_{\text{corr}}$ would need to be repeated.

## 4. Conclusions

In this paper the procedures used to calibrate our HP-DSC system have been presented in detail. Our results obtained for indium and tin samples have been compared to the results in the literature and used to construct a calibration diagram for the temperature calibration over the full range of pressure from 50 MPa up to 500 MPa. This allows the determination of the corrected temperature from the measured temperature for a thermal event occurring at any pressure.

In addition, the calibration can be checked online during an experiment by observing the temperature of the "exothermic" melting peak of a small sample of indium placed in the reference cell, and making use of the experimental result that the difference in temperature between the extrapolated onset of the endothermic melting peak for a sample of indium in the sample cell and the temperature of the maximum of the "exothermic" melting peak of a sample of indium placed in the reference cell remains essentially constant for all pressures. We describe this as an "online" calibration check.

To complete the calibration procedure, the heat calibration has been performed to determine a dimensionless enthalpy correction factor $R_{\text{corr}}(p)$ which may be used to correct all the measured enthalpy (peak area) values in our temperature range to provide a corrected enthalpy value at any given pressure value $\Delta H_{\text{corr}}(p)$.

## Acknowledgements

The authors thank Professor Lemstra and his team from the Eindhoven University of Technology, in particular W.K. Gerritsen, for technical support and helpful discussions and the UK Engineering and Physical Sciences Research Council (EPSRC) for financial support.

## References

[1] K. Blankenhorn, G.W.H. Höhne, Thermochim. Acta 187 (1991) 219–224.
[2] G.W.H. Höhne, Thermochim. Acta 332 (1999) 115–123.
[3] G.W.H. Höhne, K. Blankenhorn, Thermochim. Acta 238 (1994) 351–370.
[4] G.W.H. Höhne, J.E.K. Schawe, A.I. Shulgin, Thermochim. Acta 296 (1997) 1–10.
[5] S. Rastogi, G.W.H. Höhne, A. Keller, Macromolecules 32 (1999) 8897–8909.
[6] S. Vanden Eynde, V.B.F. Mathot, G.W.H. Höhne, J.W.K. Schawe, H. Reynaers, Polymer 41 (2000) 3411–3423.
[7] G.W.H. Höhne, S. Rastogi, B. Wunderlich, Polymer 41 (2000) 8869–8878.
[8] S. Rastogi, C.S.J. Corstjens, G.W.H. Höhne, Macromol. Symp. 166 (2001) 35–42.
[9] C.S.J. van Hooy-Corstjens, G.W.H. Höhne, S. Rastogi, Macromolecules 38 (2005) 1814–1821.
[10] D. Dalmazzone, M. Kharrat, V. Lachet, B. Fouconnier, D. Clausse, J. Therm. Anal. Calorim. 70 (2002) 493–505.
[11] B.K. Sharma, A.J. Stipanovic, Thermochim. Acta 402 (2003) 1–18.
[12] P. Le Parlouër, C. Dalmazzone, B. Herzhaft, L. Rousseau, C. Mathonat, J. Therm. Anal. Calorim. 78 (2004) 165–172.
[13] A. Seeger, D. Freitag, F. Freidel, G. Luft, Thermochim. Acta 424 (2004) 175–181.
[14] J. Köplinger, G. Kasper, S. Hunklinger, J. Chem. Phys. 113 (2000) 4701–4706.
[15] J.T. Bendler, J.J. Fontanella, M.F. Shlesinger, M.C. Wintersgill, Electrochim. Acta 46 (2001) 1615–1621.
[16] P. Papadopoulos, G. Floudas, I. Schnell, H.-A. Klok, T. Aliferis, H. Iatrou, N. Hadjichristidis, J. Chem. Phys. 122 (2005) 224906–224909.
[17] G.A. Schwartz, E. Tellechea, J. Colmenero, A. Alegría, J. Non-Cryst. Solids 351 (2005) 2616–2621.
[18] S.L. Randzio, Chem. Soc. Rev. 25 (1996) 383–392.
[19] S.L. Randzio, Thermochim. Acta 355 (2000) 107–113.
[20] M. Ribeiro, L. Pison, J.-P.E. Grolier, Polymer 42 (2001) 1653–1661.
[21] M. Wilken, K. Fisher, J. Gmehling, Chem. Eng. Technol. 25 (2002) 779–784.
[22] S.L. Randzio, Ch. Stachowiak, J.-P.E. Grolier, J. Chem. Thermodyn. 35 (2003) 639–648.
[23] M. Hess, Macromol. Symp. 214 (2004) 361–379.
[24] G. Dlubek, J. Wawryszczuk, J. Pionteck, T. Goworek, H. Kaspar, K.H. Lochhaas, Macromolecules 38 (2005) 429–437.

[25] G. Dlubek, D. Kilburn, M.A. Alam, Macromol. Chem. Phys. 206 (2005) 818–826.
[26] A.J. Pappin, M.D. Ingram, J.M. Hutchinson, G.D. Chryssikos, E.I. Kamitsos, Phys. Chem. Glasses 36 (1995) 164–171.
[27] M.D. Ingram, B. Macmillan, A.J. Pappin, B. Roling, J.M. Hutchinson, Solid State Ionics 105 (1998) 103–107.
[28] P.W.S.K. Bandaranayake, C.T. Imrie, M.D. Ingram, Phys. Chem. Chem. Phys. 4 (2002) 3209–3213.
[29] Z. Stoeva, C.T. Imrie, M.D. Ingram, Phys. Chem. Chem. Phys. 5 (2003) 395–399.
[30] M. Duclot, F. Alloin, O. Brylev, J.-Y. Sanchez, J.-L. Souquet, Electrochim. Acta 50 (2005) 5015–5021.
[31] L. Li, C. Wang, R. Huang, L. Zhang, S. Hong, Polymer 42 (2001) 8867–8872.
[32] M.C. García Gutiérrez, D.R. Rueda, F.J. Baltá Calleja, N. Stribeck, R.K. Bayer, J. Mater. Sci. 36 (2001) 5739–5746.
[33] M.C. García Gutiérrez, D.R. Rueda, F.J. Baltá Calleja, N. Stribeck, R.K. Bayer, Polymer 44 (2003) 451–455.
[34] J. Zhang, H.F. Zhang, M.X. Quan, Z.Q. Hu, Mater. Lett. 58 (2004) 1379–1382.
[35] G.W.H. Höhne, W. Dollhopf, K. Blankenhorn, P.U. Mayr, Thermochim. Acta 273 (1996) 17–24.
[36] M.L. McDaniel, S.E. Babb, G.J. Scott, J. Chem. Phys. 37 (1962) 822–828.
[37] R. Sandrock, Differential kalorimetrie (DSC) bei hohen Drücken, Dissertation, Ruhr-Universität Bochum, 1982.
[38] H. Preston-Thomas, Metrologia 27 (1990) 3–10.